Selective ring opening of decalin over bifunctional RuS2/zeolite catalysts

N. Catherin, E. Blanco, L. Piccolo, D. Laurenti, F. Simonet, C. Lorentz, E. Leclerc, V. Calemma, C. Geantet

Catalysis Today 323 (2019) 105–111

Contents lists available at ScienceDirect

Catalysis Today

journal homepage: www.elsevier.com/locate/cattod

Selective ring opening of decalin over bifunctional RuS_2/zeolite catalysts

N. Catherin[a], E. Blanco[a], L. Piccolo[a], D. Laurenti[a], F. Simonet[a], C. Lorentz[a], E. Leclerc[a], V. Calemma[b], C. Geantet[a,*]

[a] Université de Lyon, Institut de Recherches sur la Catalyse et l'Environnement de Lyon (IRCELYON), UMR5256 CNRS-UCB Lyon 1, 2 Avenue Albert Einstein, 69626 Villeurbanne Cedex, France

[b] Eni S.p.A., DOW R&D Division, Via F. Maritano 26, 20097 San Donato Milanese, Italy

ARTICLE INFO

Keywords:
Selective ring opening
Ruthenium sulfide
Zeolite
Comprehensive GC
Hydrogen sulfide

ABSTRACT

The discovery of sulfur-resistant catalysts for selective ring opening (SRO) is an important challenge for refiners, considering the future legislation on cetane index of diesel fuels. In the present work, we studied the properties of RuS_2 supported on several zeolites in gas-phase decalin hydroconversion at high hydrogen pressure (5 MPa) in the presence of 0.8% H_2S concentration. Catalytic bifunctionality was investigated by changing the Ru loading or support acidity. The addition of RuS_2 strongly improved catalytic activity of an HY zeolite, decreased coke deposition and dehydrogenation and increased selectivity towards RO products. The mechanism mainly proceeds from skeletal isomerization induced by the acidity of the zeolite but the hydrogen activation properties of RuS_2 are beneficial to the activity and stability of the catalyst.

1. Introduction

Among the strategies of research in heterogeneous catalysis, the establishment of volcano curves (*e.g.* nature of the metal *versus* activity) has been often used. For a large number of reactions such volcano curves have been obtained by plotting the rate against the position in the periodic table. This methodology was used in order to investigate new types of active phases but also to rationalize the selection of active phases from correlations with thermodynamic or electronic descriptors [1]. In hydrodesulfurization or more generally hydrotreating reactions, these periodic trends have been investigated first on unsupported sulfides by Pecoraro and Chianelli [2] for DBT hydrodesulfurization and later on by many authors for numerous reactions and model compounds (HDN, Hydrogenation…) as well as types of supports [3–7]. These systematic studies revealed the prominent activity of RuS_2 pyrite phase and led to many studies on RuS_2 on alumina, as reviewed by De los Reyes [8]. The use of a zeolite support allowed stabilizing very small particles of pyrite structure [9–11]. This combination led to very effective catalysts for aromatic hydrogenation and the active phase, stabilized by the zeolites framework, was demonstrated to be a pyrite structure with S-depleted planes [12]. These outstanding properties led us to investigate RuS_2/zeolite bifunctional catalysts for selective ring opening (SRO) of decalin, a molecule which is considered as an excellent probe for SRO of middle distillates such as LCO [13].

SRO is a promising route for increasing cetane index in diesel fuels. It is a special case of hydrocracking for which carbon-carbon bond in a naphtene is to be broken without cracking [14]. New strategies for designing efficient catalysts are required [15].The impact of SRO on cetane number (CN) was estimated using an artificial neural network program providing a predicted CN of numerous molecules of decalin SRO [15,16]. This study clearly illustrated the need of highly selective bifunctional catalysts. Concerning metal catalysts, the early works of F. Gault on 6-membered-ring compounds [17] complemented by the study of Mc Vicker et al. on bicyclic compounds evidenced the specific properties of Pt and Ir for hydrogenolyis of endocyclic C—C bonds [18]. These studies orientated this topic toward bifunctional catalysts based on Ir or Pt supported on zeolites or amorphous silice-alumina with tuned acidity, leading to performing systems [19–21] which were further proved to be efficient for increasing CN of an hydrogenated LCO [22]. However, their low thioresistance and the cost of noble metals are detrimental to their industrial application. Therefore, several attempts have been made for developing SRO catalysts which can accommodate the presence of a few percents H_2S. Hydrocracking-like catalysts such as NiWS/Al_2O_3-USY [23] NiWS/ASA catalyst [24] and NiMoS on ASA or Y zeolite [25] have been investigated with tetralin or decalin as model molecules. However, the performances remain low and the specific properties of RuS_2 on zeolites observed in hydrogenation reactions suggest that this combination of catalytic functions might be useful for SRO reactions. Therefore, we investigated the mechanism of conversion of decalin, the effect of RuS_2 loading on the zeolite performance, as well

* Corresponding author.
E-mail address: christophe.geantet@ircelyon.univ-lyon1.fr (C. Geantet).

https://doi.org/10.1016/j.cattod.2018.07.052
Received 20 April 2018; Received in revised form 20 July 2018; Accepted 28 July 2018
Available online 30 July 2018
0920-5861/

as the impact of the acidic support nature.

2. Experimental

2.1. Materials preparation

A RuS_2/HY catalyst was prepared by incipient wetness impregnation (IWI) with 3.4 wt% of ruthenium target loading ($Ru(NH_3)_6Cl_3$) (mixture matured for 8 h at room temperature and dried at 100 °C overnight). The metal salt was dissolved in 2.5 ml of distillate water and 2 g of zeolite was added. The mixture was matured for 8 h at room temperature and then was dried at 100 °C overnight. One part of as prepared Ru/HY catalyst was reduced under H_2 at 400 °C for 2 h. Another fraction was sulfided at 400 °C for 4 h under 15% H_2S/N_2 gas flow. Early works on RuS_2 based catalysts evidenced the importance of activation mixture on the catalytic performances and the necessity to use H_2S instead of H_2/H_2S mixture [26]. H_2S generates the pyrite structure which contains S_2^{2-} pairs which easily activate hydrogen [27]. A series of catalysts with different Ru loadings (0.5, 1.1 and 2.8 wt %) was also prepared by this method. The HY zeolite used (Alfa Aesar, 45866) had the following characteristics: S_{BET} = 781 m^2/g, porous volume 0.29 cm^3/g, Si/Al atomic ratio = 2.6, 1.8 wt% Na.

A second series of catalysts was prepared by IWI with nearly 3 wt % of Ru on various zeolites. Table 1 summarizes the origin and characteristics of these supports. Drying and sulfidation procedures were identical as those described for RuS_2/HY catalysts.

2.2. Catalyst characterization

High-resolution transmission electron microscopy (TEM) was performed with a 200 kV JEOL 2010 (LaB_6 filament) microscope with point-to-point resolution of 0.195 nm, and equipped with a LINK-INCA energy dispersive X-ray (EDX) analyzer. Thin cuts of the powder were made by embedding the freshly sulfide catalysts in an epoxy resin and cutting them with an ultra microtome equipped with a diamond knife. Ultrathin slices (10–50 nm) of sample grains were examined.

Textural properties were determined after degassing the samples at 473 K during 3 h. The specific surface areas were determined by nitrogen adsorption at 77 K using BET equation (ASAP 2020 – Micromeritics).

A ThermoScientific Flash 2000 analyzer was used to determine C, H, O, N and S contents. Other elemental analyses (metals) were performed by ICP-OES, after dissolution of the samples in acidic solutions, using an Activa apparatus from Horiba Jobin Yvon.

The acidity of the catalyst supports and some of supported RuS_2 catalysts was analysed by Fourier-Transform infrared spectroscopy (FTIR) of adsorbed pyridine. The concentrations of Brönsted and Lewis acid sites (per g of catalyst or per µmol of Al) after desorption at 150, 250 and 350 °C were calculated using the extinction coefficients ε_{BA} (1.67) and ε_{LA} (2.22) determined by Emeis et al. [28].

Table 1
Characterisitics of the catalyts.

Support and supplier (Reference)	BET surface area (m^2/g)	External surface area (m^2/g)	Si/Al atomic ratio	Al content wt%	Ru loading (wt%)
HY Alfa Aesar (45866)	781	51	2.6	9.6	0.5/1.1/2.8
USY-56 Zeolyst (CBV 760)	650	180	27.6	1.2	2.7
USY-200 Tosoh (HSZ 390 HUA)	822	94	132	0.3	2.8
Na(H)Y Eni	630	308	31.4	1.2	3.0
H-β TOSOH (HSZ 940 HOA)	623	60	17.7	2.0	2.9
NaCs(H)-β Eni	521	145	13.7	2.3	3.2
ASA SASOL (SIRAL-40)	423	–	0.48	36	2.7

2.3. Catalyst testing

The catalyst performances were evaluated in gas-phase decalin hydroconversion in the presence of H_2S using the high-pressure flow-fixed bed set-up already described in Ref. [23]. Two mass flow controllers (Brooks 5850TR) allow feeding pure H_2 (0–500 ml/min) and concentrated H_2S/H_2 (10% H_2S, 0–100 ml/min). The hydrocarbon partial pressure is generated by flowing H_2 through a saturator/condenser system filled with decalin (decahydronaphthalene, mixture of *cis* and *trans* isomers, Sigma-Aldrich, 98%) and maintained at appropriate temperatures by external heating. A saturator is filled with decalin at a condensation temperature of 130 °C which ensures a decalin partial pressure of 19 kPa. A secondary 10% H_2S/H_2 flow was fed to the reactor downstream the saturator to produce 0.8% H_2S concentration. The total pressure (5 MPa) was controlled by a back-pressure regulator. The U-shaped, a stainless steel reactor with an inner Pyrex tube [29] contained from 50 mg (mixed with crushed quartz) to 200 mg (pure) of packed catalyst powder. The temperature is measured by means of a thermocouple placed close to the catalytic bed. A catalytic run is performed during 20 h.

At the reactor outlet, the gas mixture is fed to an on-line Agilent 7820 A gas chromatograph equipped with a Agilent CP-Sil Pona column (150 m × 250 µm × 1 µm, H_2 as carrier gas). Two methods have been established: a fast one (28 min analysis) which gives a rapid overview of the conversion of the *cis/trans* decalin and of the stability of the catalysts and a slow one (4h15) adapted from Ref. [30].This online analysis provides decalin conversion by measuring the by-pass *cis* + *trans* decalin peaks area, and the cracking products distribution.

$$X_{dec} = \frac{(Dec_{(by-pass)} - Dec_{(out)})}{Dec_{(by-pass)}}\% \quad (1)$$

Cracking selectivity is also calculated at this stage, in order to include light (gaseous) products in the mass balance, only condensed liquids being measured by off-line GCxGC analysis (see below). The cracking product family (CkP) consists of C_1-C_9 compounds; *n*-nonane retention time has been used to mark the division between C_{10} isomers and CkP series (Eq. (2)), this compound being among the last C_9 to elute from the reactive mixture of decalin ring-opening reaction products and to be unambiguously identified [31].

$$S_{CkP} = \frac{A_{peaks,\ \ t < nonane}}{A_{peaks,\ \ tot}} \quad (2)$$

The ring-opening products (ROP) selectivity S_{rop} was obtained from the selectivity of C10 isomers and the distribution of C10 compounds obtained by GCxGC analysis.

Considering a pseudo first order for decalin, reaction rates (mol s^{-1} g^{-1}) were calculated from the following formula:

$$r_{Dec} = F_{dec} \times \frac{[-ln(1-X_{Dec})]}{m_{cata}} \quad (3)$$

where F_{dec} represent the flow of decalin, m_{cata} the catalyst mass. The rate of ROP r_{rop} was the product of S_{rop} with R_{dec}.

Even if a high resolution column is used in 1D GC, in the C_{10} zone, co-elution of isomerization and ring-opening products occurs. Therefore, a comprehensive analysis of these products was performed off-line with a GC × GC system implemented on an Agilent 6890 N chromatograph with a liquid N_2-cooled loop modulator ZX1 (Zoex Corporation). It was connected either to a mass detector (Agilent 5975B, mass range: 50–300 g/mol, up to 22 scans/sec) [32] for identification or a flame ionization detector (FID) for quantification. The

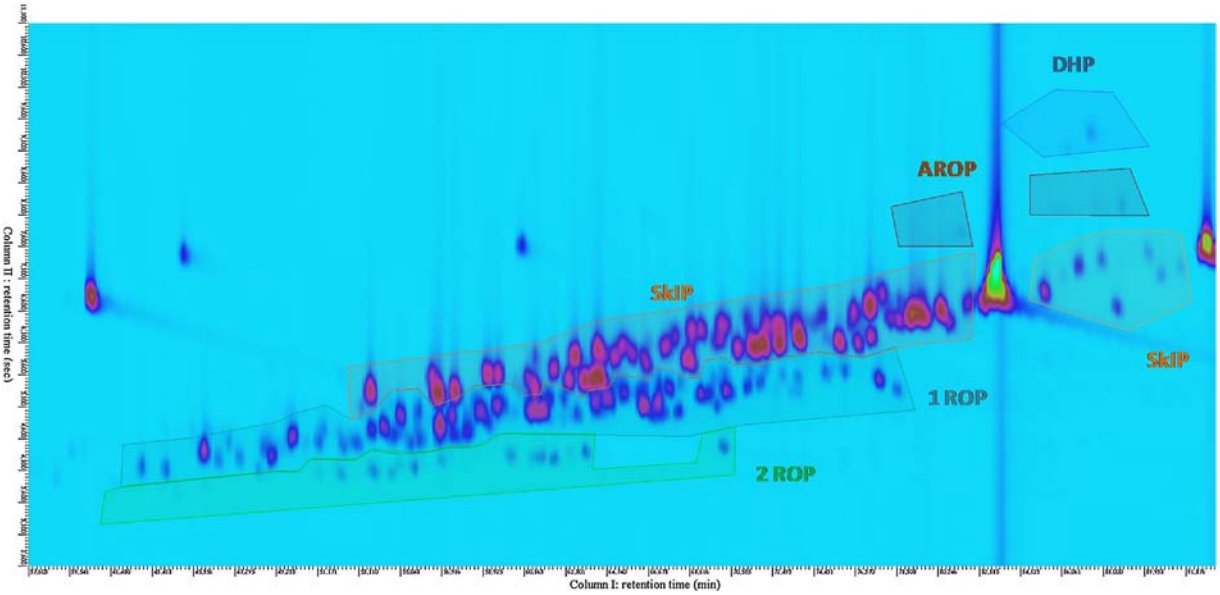

Fig. 1. Enhanced view of GC × GC chromatogram of decalin converted at 220 °C on RuS_x/HY (X = 24%, 72%SkIPs, 23%ROPs, 1% 2ROPs).

reactions lead to several products families:

SkIPs: skeletal isomerization products, *i.e.* C10 alkyl-dinaphthenes;

1ROPs: 1-ring-opening products, *i.e.* C10 alkyl-mononaphthenes;

2ROPs: 2-ring-opening products, *i.e.* C10 paraffins;

DHPs: dehydrogenation products, *i.e.* all C10 unsaturated products except AROPs (tetralin, naphthalene, methyl-indans, *etc.*).

AROPs: aromatic 1-ring-opening products, *i.e.* C10 alkyl-benzenes;

The dominant ones are skeletal-isomerization products (SkIPs) and ring-opening products (ROPs- 1 or 2 rings opening) with a small contribution of 2ROPs. GC × GC technique can unambiguously discriminate between all these C_{10} SkIPs and ROP products [33]. We have recently demonstrated that comprehensive GC × GC–MS can achieve an entire description of the C_{10} products formed, and GC × GC FID permits their quantification. Analytical details can be obtained from Ref. [34]. An example of a GC × GC chromatogram is given in Fig. 1.

3. Results and discussion

3.1. Impact of the presence of RuS_x on the catalytic performance

The selectivities obtained with HY support, reduced Ru/HY and RuS_x/HY at nearly 50% conversion of decalin, at 300 °C, and in the presence of H_2S are compared in Fig. 2 and the rates of conversion of decalin and ring opening rates are summarized in Table 2. HY zeolites

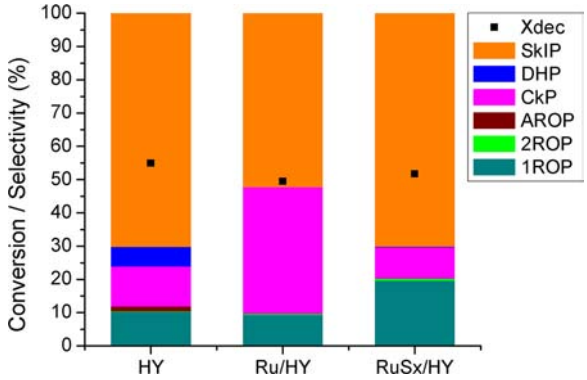

Fig. 2. Conversion and selectivities for decalin hydroconversion over HY, Ru/HY and RuS_x/HY catalysts measured at 300 °C and WHSV of respectively 0.6,0.6, 5.9 h^{-1} (conversion close to 50%).

Table 2
Catalytic performance of HY based catalysts in decalin conversion at 300 °C.

Catalyst	HY	Ru/HY	Ru/HY
r_{dec} (10^{-8} mol g^{-1} s^{-1})	84	73	152
r_{rop} (10^{-8} mol g^{-1} s^{-1})	10	7	152

alone can catalyze SRO reaction but a strong deactivation occurred during the first hours of the reaction. Various zeolites (Hβ, Mordenite, H − MCM 41, HY-12) have been already investigated in the ring opening of decalin by Kubicka et al. [35].These authors evidenced the need of skeletal isomerisation before ring opening and the crucial role of Brönsted (B) sites. The strongest Brönsted sites induced a rapid deactivation. A similar trend was observed during the conversion of decalin isomers on a series of HY zeolites by Santikunaporn et al. [36]. In our case, with HY zeolites, after 5 h on stream, half of the initial conversion was lost indicating coke deposition. After 72 h, 16 wt% of C was analysed on the used HY. On the contrary, RuSx/HY catalyst remains stable from the beginning of the test, nevertheless 11 and 9 wt% of C were found after test on 3.4 and 1 wt% Ru catalysts respectively. This also suggest that strongest acid sites are probably coked with time on stream. The fact that the zeolite alone is active for ring opening indicates that hydrogen activation occurs. This has been attributed to several origins such as alkali metal cations, iron impurities or Brönsted acid sites and depends on PH_2 and reaction temperature [37]. The use of reduced Ru, strongly enhances cracking and is detrimental to SRO. The distribution of light products is characteristic of cationing hydrocracking mechanism (M shape) [14]. In fact, the introduction of much lower H_2S partial pressure is detrimental to the hydrogenolytic properties of the metal as it has been demonstrated in the case of Ir on zeolites [34]. This catalyst was therefore not studied further. In fact, in the presence of H_2/H_2S mixture, the resulting poisoned catalysts loses its hydrogenolytic properties but has also weaker hydrogenation properties as compared to the bare metal or the pyrite RuS_2 [27].

The comparison of reaction rates demonstrates that the introduction of RuS_2 drastically increases the rate of conversion but also doubles the selectivity towards ROPs. In order to investigate the reaction mechanism, we studied the evolution of products in a wider range of conversion. Thus, the reaction was also performed at 240 °C and the evolution of the selectivity as a function of the conversion for RuS_2/HY and HY is illustrated in Fig. 3. Thermodynamically, it has been shown

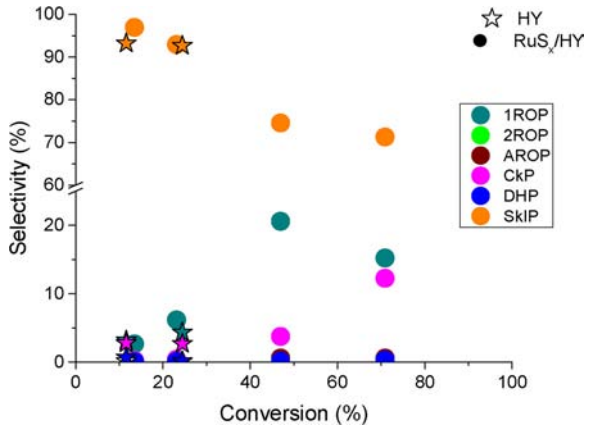

Fig. 3. Evolution of selectivities with decalin conversion at 240 °C, on HY (open circles) and RuS_x/HY (full circles).

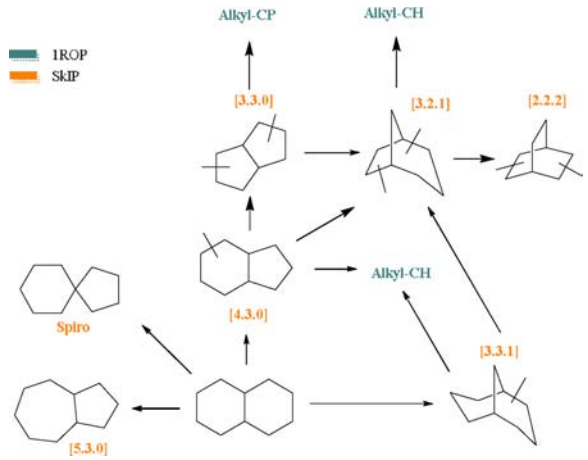

Scheme 1. Reaction pathway proposed for early stages of decalin conversion over RuS_x/HY catalyst.

by Govindhakannan et al. [38] that low reaction temperatures favour the formation of RO products and reduces cracking. As compared to other sulfide catalysts systems, RuS_2/HY bifunctional catalysts is efficient below 300 °C.

From these data, it is clear that reaction proceeds through a consecutive mechanism with, at first, the formation of Skips, followed by ROPs and cracking products. The switch from ROPs to SkIPs as main products upon metal sulfidation was recently demonstrated for Ir/HY [32]. The molecular details of the distribution of SkIPs and ROPs obtained from the three samples, at 300 °C, are shown in Fig. 3. The main products observed are various C_{10} isomers, belonging to so-called [4.3.0], [3.3.0] and [3.2.1] groups, which are presented in Scheme 1 . UkPs refers to a few unidentified compounds.

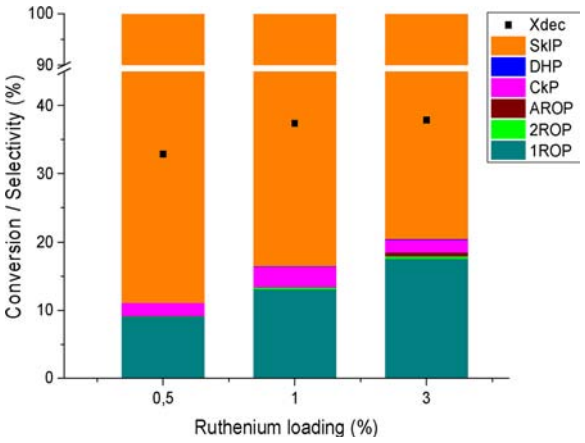

Fig. 5. Effect of Ru loading on products distribution for decalin hydroconversion at 240 °C and *ca.* 35% conversion.

Table 3
Evolution of catalytic properties and average particle size and content with Ru loading.

Ru loading wt%	0.5	1.1	2.8
r_{dec} (10^{-8} mol g^{-1} s^{-1})	83	123	76
r_{rop} (10^{-8} mol g^{-1} s^{-1})	8	17	14
Particle size (nm)	1	0.8	1.4
Number of particles of RuS_2 (10^{17} part/$g_{catalyst}$)	1.4	4.5	2.2

This Scheme 1 describes the first stages of the reaction. The main route passes through (branching) type B isomerization and the formation of [4.3.0] compounds, which favors later on the formation of alkylated ROPs with shorter chains. A parallel, though minor route, type A isomerization, produces other bicyclic compounds such as spirodecane [19].

This type A pathway favors longer chain ROPs. 1ROPs can either contain a five-membered ring (CP) or a six-membered ring (CH). Fig. 4 (bottom) provides the ROP distribution according to the length of the longest alkyl chain attached to the ring. As already discussed for SkIPs, the main ROPs are propyl or ethyl ones. The products distributions at the molecular level for the bare support and Ru-based catalysts are similar. This clearly indicates that the mechanism observed is driven by the acidic properties of the zeolites and corresponds to the one proposed by Kubicka et al. [35]. However, the combination with RuS_2 enhances by ten times the catalytic ROP activity and the stability (see Supplementary S1) of the catalyst as compared to HY alone. Therefore, we attempted to modify the RuS_x content in order to estimate the effect of the balance between acidic and hydrogenating sites.

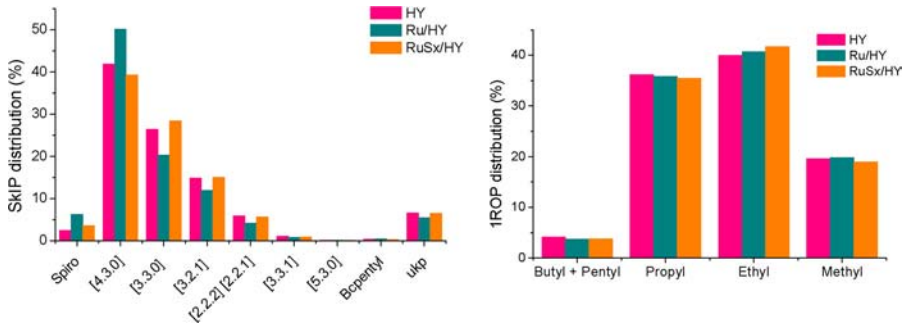

Fig. 4. Distribution of SkIPs (top) and ROPs (bottom) for HY, Ru/HY, and RuS_x/HY catalysts at 300 °C and close to 50% conversion (Cf Fig. 2).

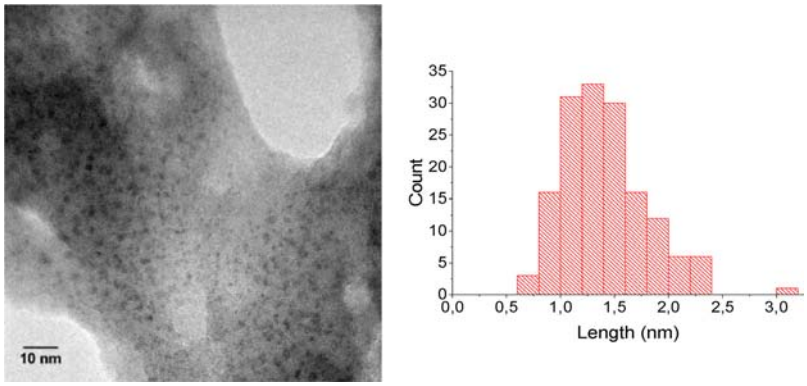

Fig. 6. TEM picture and particle size distribution of 3.4 wt% RuS_2/HY (IWI) sample.

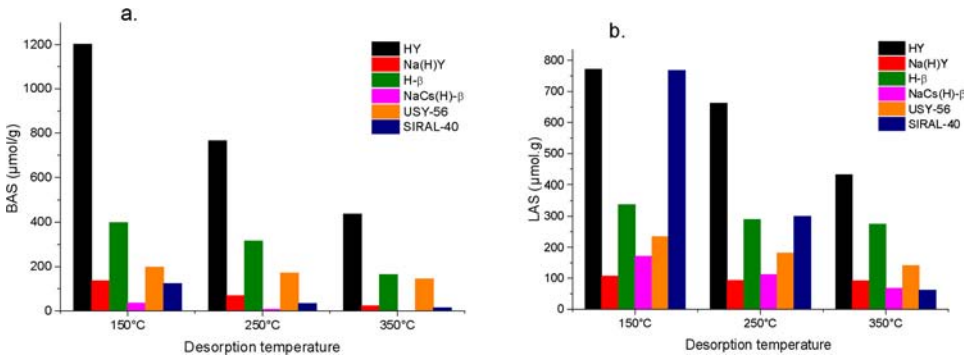

Fig. 7. Quantification of Brønsted (a) and Lewis acid sites (b) of the zeolite supports from pyridine IR at various desorption temperatures.

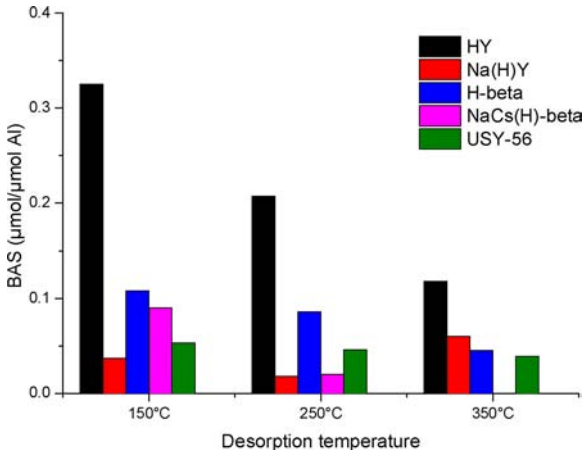

Fig. 8. Quantification of Brønsted sites expressed by µmol of Al contained in the zeolites.

Table 4
Rate of conversion of decalin and ROPs formation for RuSx supported catalysts at 300 °C. (Ru metals loading are reported in Table 1).

Acidic support	r_{dec} (10^{-8} mol g^{-1} s^{-1})	r_{rop} (10^{-8} mol g^{-1} s^{-1})
H-β	845	114
USY-56	65	10
Na(H)Y	53	6
Siral 40	23	2
Na(Cs) H-β	26	3
USY-200	29	2

3.2. Impact of RuS_2 loading

Fig. 5 reports the catalytic performances for three Ru loadings. At 240 °C and similar conversion levels (*ca.* 35%) and Table 3. summarizes the catalytic performances. An optimum was reached at 1% probably due to a higher dispersion of the particles. However, the highest Ru loading leads to the highest RO selectivity.

The bifunctional characteristics of the catalysts have been investigated with physicochemical methods. IR of pyridine on HY zeolite, desorbed at 250 °C, measures concentrations of Lewis (L) and Brönsted (B) sites of 662 and 766 µmol/g, respectively. The range of RuS_x particle size (see Table 3) explain the over-stoichiometric $RuS_{2.8}$ phase observed on the fresh catalyst by chemical analysis or EDX. This over-stoechiometry is due to the complete coordination of Ru atoms by sulfur pairs of RuS_2 nanoparticles [39].

The average RuS_2 particle size of the catalyst series with increasing Ru loading are reported in Table 3. The interaction with the zeolites stabilizes particle in the range of 1 to 2 nm. Fig. 6 shows the distribution of the RuS_2 particles on the zeolites and the particle size distribution (the other size distributions are provided in S4). Considering a simple geometrical model of pyrite structure, one can estimate the number of particles per g of catalyst (see Table 3). The highest amount of particles as well as activity was obtained with the 1 wt% loading catalyst suggesting better balance between the hydrogenation sites of the sulfide and the acidic sites of the zeolites. The RuS_2 phase is also partially reduced under catalytic conditions since S/M decreased from 2.8 in the fresh state to 1.2 in the used one. This has been observed in several cases, for instance for hydrogenation reaction, and it has been proposed from XAS experiments that particles are composed + of RuS_2 cores and some metal-like domains at the surface [12,40]. However, as it was demonstrated above with the experiment using a pre-reduced catalyst, the presence of pyrite-type sulfur is required for an efficient bifunctional catalyst. These metal-like structures may contribute to the adsorption of the reactant whereas S_2^{2-} entities favour H_2 activation

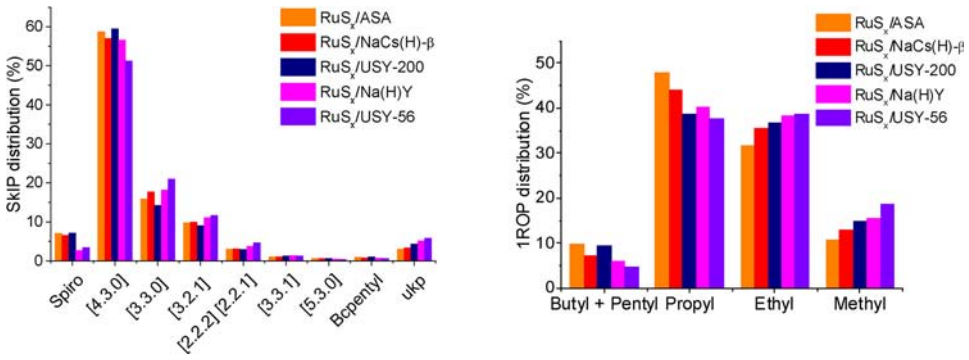

Fig. 9. Distribution of Skips (left) and ROPs (right) for decalin hydroconversion over RuS_2 supported on modified HY, H-β and ASA supports (20–25% conversion, 300 °C).

[41].

3.3. Impact of the support nature and acidity

Since the sulfide phase content has a small impact on the performance of the bifunctional catalyst, we attempted to optimize the acidic function. As it has been illustrated with metals such as Ir or Pt, acid/metal site ratio is crucial for improving ROP selectivity [42] and a careful control of the acidic properties can reveal the hydrogenolytic function of the noble metals and orient the reaction towards the desired ROPs instead of isomerized ones [22,43]. Therefore, the acidic properties of the series of supports presented in Table 1 were investigated by pyridine IR. Fig. 7 summarizes these properties in terms of total amount of L or B sites. Three categories of supports can be classified according to the concentration of acid sites per g of catalysts. High acidic content (HY and H-β), average acidity (USY-56, Na(H)Y) and small acidity NaCs (H)-β, USY 200 and ASA. As suggested by Busca and col. [44,45], when Al content is low, the amount of B sites depends on Al concentration. Therefore, the strength of these acid sites of the zeolite series can be also illustrated by reporting the concentration per μmol of Al (without considering extra framework species) as presented in Fig. 8. The ranking is slightly different, since the two beta zeolites have comparable content of B sites after desorption at 150 °C but NaCs(H)-β B acidity strength is weaker. Acidity was also determined for three sulfide catalysts (RuS_2 3% and 1% and RuS_2/USY 56). Slights modifications on L and B sites are observed but the ranking of overall acidity between was kept (see SI). In fact, introduction of RuS_2 on the acidic supports slightly modifies the acidity of the system since on the one side some sites are consumed upon impregnation but on the other side RuS_2 present also some acidic properties revealed by IR of pyridine [46] or CO [iv,47]. The overall trend suggests that higher the amount of acid sites is, better the catalyst is.

The comparison of the catalytic properties at 300 °C (see Table 4) evidenced that RuS_2/H-β exhibits a behavior close to that of RuS_2/HY with r_{dec} (see Table 2) but with a cracking rate twice higher. At iso-conversion, the distributions of SkIPs and ROPs are similar. RuS_x deposited on medium acidic catalyst (USY-56, Na(H)Y) are less active with r_{dec} in the range of 50–60 10^{-8} mol g^{-1} s^{-1} (r_{rop} = 6–10 10^{-8} mol g^{-1} s^{-1}) and on the weakly acidic catalysts, r_{dec} drops to 20–30 10^{-8} mol g^{-1} s^{-1} and r_{rop} decreases t 2 10^{-8} mol g^{-1} s^{-1}.

Therefore, we can conclude that a high acidity is needed to perform the reaction. Note that Na(H)Y and NaCs(H)-β supports were those showing the highest performances when loaded with noble metals and in the absence of sulfur [21,27]. The decrease of B sites strength for NaCs(H)-β (desorption at 250 °C on Fig. 8), as compared to H-β, seems to be mandatory for catalysts performance. The products distributions of these less active catalysts are compared at 20–25 % conversion in Fig. 9. We can notice the main trends already observed for RuS_2/HY sample (see Fig. 3) with almost the same distribution of SkIPs and ROPs. However, slight variations such as more methylated compounds with the most acidic supports are seen (see Fig. 8 and Supplementary S2).

Thus, we illustrate again that the driving force of ring opening of decalin is the amount of acidic sites with a relatively high strength. The RuS_2 average particle sizes determined by HRTEM varied from 1.2 nm for ASA up to 3 nm for USY-56 and low acidic catalysts exhibit a high ratio of RuS_2 particles per OH group but with no favourable impact on the catalytic performance.

4. Conclusions

Whereas RuS_2 is well known to efficiently break the C–S bond, it does not seem to be able to catalyze the hydrogenolysis of endocyclic C—C bonds. However, ring opening of decalin can be achieved, under H_2S partial pressure, at relatively low temperature (200–250 °C) over RuS_2/zeolites bifunctional catalysts. The introduction of RuS_2 on a HY zeolite greatly improves the rate of conversion of decalin as well as the stability of the catalyst. Even in the presence of 0.8% of H_2S, concentration level which poisons the metal catalysts, high conversion levels can be reached at relatively low temperature (250 °C) in the presence of H_2S. This has to be compared for instance with NiWS/ASA catalysts, which required a temperature of 350 °C for catalyzing the same reaction [23]. We attempted to optimize the metal sulfide and acidic functions, either by modifying metal loading or support acidity. As a result, the total acidity of the zeolites appears to govern the catalyst reactivity toward decalin, most performing catalysts were obtained with the $_{RuS2}$ deposited on the unmodified acidic zeolites (HY or Hβ) . 1 wt %Ru loading seems to be an optimum for the catalytic performances.

Acknowledgements

N. C. and E. B. thanks Eni SpA for financial support.

This special issue is dedicated to Pr U. Ozkan. We cannot tell the precise moment when friendship is formed. With Umit and Erdal, our opportunities to meet were every time instants of intimacy and kindness.

Appendix A. Supplementary data

Supplementary material related to this article can be found, in the online version, at doi:https://doi.org/10.1016/j.cattod.2018.07.052.

References

[1] H. Toulhoat, P. Raybauld, J. Catal. 216 (2003) 63.
[2] T.A. Pecoraro, R.R. Chianelli, J. Catal. 67 (1981) 430.
[3] M. Lacroix, N. Boutarfa, C. Guillard, M. Vrinat, M. Breysse, J. Catal. 120 (1989) 473.
[4] J.P.R. Vissers, C.K. Groot, E.M. Van Oers, V.H.J. De Beer, R. Prins, Bull. Soc. Chim.

Belg. 93 (1984) 813.
[5] J. Ledoux, O. Michaux, G. Agostini, J. Catal. 102 (1986) 275.
[6] S. Eijbouts, V. de Beer, R. Prins, J. Catal. 109 (1988) 217.
[7] J. Quartararo, S. Mignard, S. Kasztelan, J. Catal. 192 (2000) 307.
[8] J.A. De Los Reyes, Appl. Catal. A 322 (2007) 106.
[9] V. Kougionas, M. Cattenot, J.L. Zotin, J.L. Portefaix, M. Breysse, Appl. Catal. A 124 (1995) 153.
[10] M. Breysse, M. Cattenot, V. Kougionas, J.C. Lavalley, F. Mauge, J.L. Portefaix, J.L. Zotin, J. Catal. 168 (1997) 143.
[11] C. Sun, M.-J. Peltre, M. Briend, J. Blanchard, K. Fajerwerg, J.-M. Krafft, M. Breysse, M. Cattenot, M. Lacroix, Appl. Catal. A 245 (2002) 245.
[12] B. Moraweck, G. Bergeret, M. Cattenot, V. Kougionas, C. Geantet, J.L. Portefaix, M. Breysse, J. Catal. 165 (1997) 45.
[13] A. Corma, V. González-Alfaro, A.V. Orchillés, J. Catal. 200 (2001) 34.
[14] J. Weitkamp, ChemCatChem 4 (2012) 292.
[15] P.T.M. Do, S. Crossley, M. Santikunaporn, D.E. Resasco, J.J. Spivey, K.M. Dooley (Eds.), Catalysis, vol. 20, RCS Publishing, 2007, p. 33.
[16] R.C. Santana, P.T. Do, M. Santikunaporn, W.E. Alvarez, J.D. Taylor, E.L. Sughrue, D.E. Resasco, Fuel 85 (2006) 643.
[17] F.G. Gault, Adv. Catal. 30 (1981) 1.
[18] G.B. Mc Vicker, M. Daage, M.S. Touvelle, C.W. Hudson, D.P. Klein, W.C. Baird, B.R. Cook, J.G. Chen, S. Hantzer, D.E.W. Vaughan, E.S. Ellis, O.C. Feeley, J. Catal. 201 (2002) 137.
[19] S. Rabl, A. Haas, D. Santi, C. Flego, M. Ferrari, V. Calemma, J. Weitkamp, Appl. Catal. A 400 (2011) 131.
[20] S. Rabl, D. Santi, A. Haas, M. Ferrari, V. Calemma, G. Bellussi, J. Weitkamp, Microporous Mesoporous Mater. 146 (2011) 190.
[21] S. Nassreddine, S. Casu, J.L. Zotin, C. Geantet, L. Piccolo, Catal. Sci. Technol. 1 (2011) 408.
[22] V. Calemma, M. Ferrari, S. Rabl, J. Weitkamp, Fuel 111 (2013) 763.
[23] L. Wang, B. Shen, F. Fang, F. Wang, R. Tian, Z. Zhang, L. Cui, Catal. Today 158 (2010) 343.
[24] L. Di Felice, N. Catherin, L. Piccolo, D. Laurenti, E. Blanco, E. Leclerc, C. Geantet, V. Calemma, Appl. Catal. A 512 (2016) 43.
[25] S.G.A. Ferraz, F.M.Z. Zotin, L.R.R. Araujo, J.L. Zotin, Appl. Catal. A 384 (2010) 51.
[26] Y.J. Kuo, B.J. Tatarchuk, J. Catal. 112 (1988) 229.
[27] A. Cocco, B.J. Tatarchuk, Langmuir 5 (1989) 1309.
[28] C.A. Emeis, J. Catal. 141 (1993) 347.
[29] F. Labruyère, M. Lacroix, D. Schweich, M. Breysse, J. Catal. 167 (1997) 464.
[30] A. Haas, S. Rabl, M. Ferrari, V. Calemma, J. Weitkamp, Appl. Catal. A 97 (2012) 425.
[31] S. Rabl, PhD Universität Stuttgart (2011).
[32] G. Toussaint, C. Lorentz, M. Vrinat, C. Geantet, Anal. Methods 3 (2011) 2743.
[33] L. Piccolo, S. Nassreddine, G. Toussaint, C. Geantet, J. Chromatogr. A 1217 (2010) 5872.
[34] E. Blanco, L. Di Felice, N. Catherin, L. Piccolo, D. Laurenti, C. Lorentz, C. Geantet, V. Calemma, Ind. Eng. Chem. Res. 55 (2016) 12516.
[35] D. Kubicka, N. Kumar, P. Maki-Arvela, M. Tiitta, V. Niemi, T. Salmi, D. Murzin, J. Catal. 222 (2004) 65.
[36] M. Santikunaporn, J.E. Herrera, S. Jongpatiwut, D.E. Resasco, W.E. Alvarez, E.L. Sughrue, J. Catal. 228 (2004) 100.
[37] J. Kanai, J.A. Martens, P.A. Jacobs, J. Catal. 133 (1992) 527.
[38] J. Govindhakannan, K. Chandra Mouli, Aaron Phoenix, Craig F. Fairbridge, Ajay K. Dalai, Fuel 97 (2012) 400.
[39] C. Geantet, C. Calais, M. Lacroix, C. R. Acad. Sci. Ser. 315 (1992) 439.
[40] J. Blanchard, K.K. Bando, T. Matsui, M. Harada, M. Breysse, Y. Yoshimura, Appl. Catal. A 322 (2007) 98.
[41] M. Breysse, E. Furimsky, S. Kasztelan, M. Lacroix, G. Perot, Catal. Rev. Sci. Eng. 44 (2002) 651.
[42] S. Nassreddine, L. Massin, M. Aouine, C. Geantet, L. Piccolo, J. Catal. 278 (2011) 253.
[43] D. Santi, T. Holl, V. Calemma, J. Weitkamp, Appl. Catal. A 455 (2013) 46.
[44] G. Busca, Microporous Mesoporous Mater. 254 (3) (2017).
[45] T.K. Phung, G. Busca, Appl. Catal. A 504 (2015) 151.
[46] G. Berhault, M. Lacroix, M. Breysse, F. Mauge, J.C. Lavalley, H. Nie, L. Qu, J. Catal. 178 (1998) 555–565.
[47] A. Infantes-Molina, A. Romero-Pérez, E. Finocchio, G. Busca, A. Jimenez-Lopez, E. Rodriguez Castellon, J. Catal. 305 (2013).